Published OnlineFirst March 8, 2011; DOI: 10.1158/1078-0432.CCR-10-2320

Clinical Cancer Research

Human Cancer Biology

Involvement of the TGF-β and β-Catenin Pathways in Pelvic Lymph Node Metastasis in Early-Stage Cervical Cancer

Maartje G. Noordhuis[1], Rudolf S.N. Fehrmann[1], G. Bea A. Wisman[1], Esther R. Nijhuis[1], Jelmer J. van Zanden[1], Perry D. Moerland[5,6], Emiel Ver Loren van Themaat[5], Haukeline H. Volders[1], Mirjam Kok[1], Klaske A. ten Hoor[1], Harry Hollema[2], Elisabeth G.E. de Vries[3], Geertruida H. de Bock[4], Ate G.J. van der Zee[1], and Ed Schuuring[2]

Abstract

Purpose: Presence of pelvic lymph node metastases is the main prognostic factor in early-stage cervical cancer patients, primarily treated with surgery. Aim of this study was to identify cellular tumor pathways associated with pelvic lymph node metastasis in early-stage cervical cancer.

Experimental Design: Gene expression profiles (Affymetrix U133 plus 2.0) of 20 patients with negative (N_0) and 19 with positive lymph nodes (N_+), were compared with gene sets that represent all 285 presently available pathway signatures. Validation immunostaining of tumors of 274 consecutive early-stage cervical cancer patients was performed for representatives of the identified pathways.

Results: Analysis of 285 pathways resulted in identification of five pathways (TGF-β, NFAT, ALK, BAD, and PAR1) that were dysregulated in the N_0, and two pathways (β-catenin and Glycosphingolipid Biosynthesis Neo Lactoseries) in the N_+ group. Class comparison analysis revealed that five of 149 genes that were most significantly differentially expressed between N_0 and N_+ tumors ($P < 0.001$) were involved in β-catenin signaling (TCF4, CTNNAL1, CTNND1/p120, DKK3, and WNT5a). Immunohistochemical validation of two well-known cellular tumor pathways (TGF-β and β-catenin) confirmed that the TGF-β pathway (positivity of Smad4) was related to N_0 (OR: 0.20, 95% CI: 0.06–0.66) and the β-catenin pathway (p120 positivity) to N_+ (OR: 1.79, 95%CI: 1.05–3.05).

Conclusions: Our study provides new, validated insights in the molecular mechanism of lymph node metastasis in cervical cancer. Pathway analysis of the microarray expression profile suggested that the TGF-β and p120-associated noncanonical β-catenin pathways are important in pelvic lymph node metastasis in early-stage cervical cancer. *Clin Cancer Res; 17(6); 1317–30. ©2011 AACR.*

Introduction

Standard treatment of early-stage cervical cancer patients consists of radical hysterectomy and pelvic lymphadenectomy. For this group of patients, the presence of lymph node metastases is the most important prognostic factor (1). Early-stage cervical cancer patients with negative lymph nodes have a 5-year survival of 90% versus only 65% in patients with lymph node metastases (2). Patients with lymph node metastases are therefore treated with adjuvant (chemo)radiation. However, the combination of surgery and (chemo)radiation is associated with severe morbidity (3). If the presence of metastatic lymph nodes could be predicted prior to treatment, primary chemoradiation could be considered, which is equally effective, but associated with a different treatment-related morbidity pattern.

Several histopathological characteristics such as tumor size, lymph vascular space involvement, and depth of invasion have been associated with lymph node metastases in cervical cancer but none of these is of sufficient clinical relevance (4). Furthermore, various molecular tumor markers like the expression of VEGF and p16 have been reported to be related with lymph node metastases in cervical cancer (5, 6), but presently no markers are available to predict lymph node status with high sensitivity and specificity. Non- and minimal invasive diagnostic techniques, such as sentinel lymph node biopsy are currently

Authors' Affiliations: Department of [1]Gynecologic Oncology, [2]Pathology, [3]Medical Oncology, and [4]Epidemiology, University Medical Center Groningen, University of Groningen, Groningen, The Netherlands; [5]Bioinformatics Laboratory, Department of Clinical Epidemiology, Biostatistics, and Bioinformatics, Academic Medical Center, Amsterdam, The Netherlands; and [6]Netherlands Bioinformatics Centre (NBIC), Nijmegen, The Netherlands

Note: Supplementary data for this article are available at Clinical Cancer Research Online (http://clincancerres.aacrjournals.org/).

Note: Current address of Emiel Ver Loren van Themaat: Max-Planck-Institute for Plant Breeding Research, Carl-von-Linne-Weg 10, 50829 Köln, Germany

Note: M.G. Noordhuis and R.S.N. Fehrmann contributed equally to this study.

Corresponding Authors: E. Schuuring, Department of Pathology, University Medical Center Groningen, PO Box 30001, 9700 RB Groningen, the Netherlands. Phone: 31-50-3619623; Fax: 31-50-3619107. E-mail: e.schuuring@path.umcg.nl; or G.B.A. Wisman, Department of Gynecologic Oncology, University Medical Center Groningen, PO Box 30001, 9700 RB Groningen, the Netherlands. Phone: 31-50-3619554; Fax: 31-50-3611806. E-mail: g.b.a.wisman@og.umcg.nl

doi: 10.1158/1078-0432.CCR-10-2320

Published OnlineFirst March 8, 2011; DOI: 10.1158/1078-0432.CCR-10-2320

Translational relevance

Presence of lymph node metastases is still the most important factor in the choice of treatment for early-stage cervical cancer patients. No other markers are currently available for accurate prediction of pelvic lymph node metastases. To identify cellular tumor pathways associated with lymph node metastasis, we analyzed all 285 presently available pathways, using differential expression array data and novel gene set enrichment algorithms. Interestingly, of the 285 pathway signatures, two well-known cellular tumor pathways (TGF-β pathway activation and dysregulation of the p120-associated noncanonical β-catenin pathway) were found to be predictive. Our data indicate that markers characteristic for these pathways can be used to predict presence of lymph node metastasis, which can influence treatment management in early-stage cervical cancer. More importantly, by the identification of these two pathways involved in lymph node metastasis in early-stage cervical cancer, new opportunities for pathway-targeted therapy can be considered to inhibit the metastatic potential.

being explored to better identify patients with disease outside the cervix (7).

Little is known about biological pathways involved in lymph node metastasis in cervical cancer. Metastasis is a complex, multistep process involving decreased cell–cell interaction, increased cell migration, disruption of the basal membrane, intravasation into the circulation, survival of direct exposure to the immune system and extreme mechanic forces in the bloodstream, and finally extravasation and growth in metastatic sites (8). Apart from tumor-specific changes, many processes in the tumor microenvironment of the primary tumor have shown also to be important for initiation of the metastatic potential at the primary site (9).

Gene expression profiling has provided tools to identify patterns of biological differences between different tumor types, cancers with diverse clinical outcome or treatment responses (10, 11). To get insight into the mechanism of lymph node metastasis in head and neck (12), colorectal (13), and cervical cancer (14–17), gene expression profiling has been used. However, in most studies little overlap was found between differentially expressed genes, which may be due to a variety of methodological issues (18). Explanations that have been debated extensively in the literature are the use of different microarray platforms (18, 19) and the restricted number of samples used to select genes from a large pool of probes (20). Therefore, comparing gene expression profiles with gene sets that represent unique pathways may provide more insight into the mechanism of lymph node metastasis. Different pathway analysis methods have been developed, including Gene Set Enrichment Analysis (GSEA). GSEA is used to determine whether predefined gene sets available for example in the Kyoto Encyclopedia of Genes and Genomes (KEGG; ref. 21) and Biocarta data bases (http://www.biocarta.com/), show significant, concordant differences between 2 phenotypes (22). Another method has recently been developed by Bild and colleagues (23). Experimentally generated expression signatures using human primary mammary epithelial cell cultures (HMEC) that reflect the activation of various oncogenic signaling pathways (c-Myc, H-Ras, c-Src, E2F3, and β-catenin) can be used to assess the activation probability of the oncogenic pathways in individual expression profiles. Both methods have not been applied previously for differentiating between lymph node negative and positive cervical cancer patients.

The aim of this study was to identify cellular tumor pathways associated with pelvic lymph node status in patients with early-stage cervical cancer. Apart from obtaining more insights on the molecular processes of lymph node metastasis in early-stage cervical cancer, our findings might contribute to individual treatment strategies. To identify such pathways, expression array analysis was performed on a well defined series of cervical squamous cell carcinomas of patients with histologically confirmed lymph node metastases (N_+) versus patients with histological and clinically confirmed negative lymph nodes (N_0). Potential markers representing the predictive value of pathways were validated in a large consecutive series of early-stage cervical cancer patients by immunohistochemistry on tissue microarrays (TMA).

Materials and Methods

Patients and tumor samples

Since 1980 clinicopathological characteristics of all cervical cancer patients referred to the Department of Gynecological Oncology of the University Medical Center Groningen are prospectively collected in a database. For the present study, patients with stage IB-IIA disease, primarily treated with surgery between 1980 and 2004 were selected ($n = 337$). Follow-up data were collected for at least 5 years. Staging was performed according to FIGO guidelines. Primary treatment consisted of type 3 radical hysterectomy and pelvic lymph node dissection. In case of poor prognostic factors, such as lymph node metastases or positive resection margins, patients were treated with adjuvant radiotherapy or chemoradiation. From these patients paraffin-embedded, formalin-fixed primary tumor tissue was collected. All tumor tissues were histological revised and only tumor specimens with sufficient tumor cells were included in the study for construction of the TMA. In 274 cases, sufficient pretreatment paraffin-embedded tissue was available for TMA construction. Of 274 patients, 112 (41%) received adjuvant (chemo)radiation. Median follow-up time for patients on the TMA was 5.5 years (range 0.3–18.6). Since 1990, when sufficient material was available, pretreatment fresh frozen tumor tissue was stored. For the microarray experiment, we selected fresh frozen primary cervical cancer tissue, containing at least 80% tumor

Published OnlineFirst March 8, 2011; DOI: 10.1158/1078-0432.CCR-10-2320

Table 1. Patient and tumor characteristics

	Microarray experiment Lymph node negative $n = 20$	Microarray experiment Lymph node positive $n = 19$	Tissue microarray $n = 274$
Age at diagnosis, median (range)	47.39 (31.53–72.71)	40.44 (29.10–72.51)	43.65 (23.67–84.65)
FIGO stage	n (%)	n (%)	n (%)
Ib1	11 (55)	10 (53)	174 (64)
Ib2	5 (25)	6 (32)	54 (20)
IIa	4 (20)	3 (16)	46 (17)
Histology			
Squamous cell carcinoma	20 (100)	19 (100)	182 (66)
Adenocarcinoma	0 (0)	0 (0)	74 (27)
Other	0 (0)	0 (0)	18 (7)
Grade of differentiation			
Good/moderate	15 (75)	10 (53)	163 (59)
Poor/undifferentiated	4 (20)	9 (47)	106 (39)
Unknown	1 (5)	0 (0)	5 (2)
Lymphangioinvasion			
No	14 (70)	6 (32)	132 (48)
Yes	6 (30)	12 (63)	142 (52)
Unknown	0 (0)	1 (5)	0 (0)
Infiltration depth			
0–10 mm	14 (70)	3 (16)	135 (49)
≥10 mm	5 (25)	14 (74)	126 (46)
Unknown	1 (5)	2 (11)	13 (5)
Tumor diameter			
0–4 cm	14 (70)	12 (63)	198 (72)
≥4 cm	6 (30)	7 (37)	76 (28)
Lymph nodes			
Negative	20 (100)	0 (0)	194 (71)
Positive	0 (0)	19 (100)	80 (29)

cells, of patients with histologically confirmed N_0 ($n = 20$) and of patients with N_+ ($n = 19$). The N_0 and N_+ groups were matched for age, FIGO stage, and histology (all squamous cell carcinoma). However, as expected the groups differed regarding presence of lymphangioinvasion ($P = 0.024$) and infiltration depth ($P = 0.001$). Patient and tumor characteristics are summarized in Table 1. In the University Medical Center Groningen, clinicopathologic and follow-up data are prospectively obtained during standard treatment and follow-up and stored in a computerized registration database. For the present study, all relevant data were retrieved from this computerized database into a separate, anonymous database. Patient identity was protected by study-specific, unique patient numbers. Codes were only known to 2 dedicated data managers, who also have daily responsibility for the larger database. In case of uncertainties with respect to clinicopathologic and follow-up data, the larger databases could only be checked through the data managers, thereby ascertaining the protection of patients' identity. Using the registration database all tissue specimens were identified by unique patient numbers and retrieved from the archives of the Department of Pathology. Therefore, according to Dutch law no further Institutional Review Board approval was required (http://www.federa.org/).

Microarray experiments

From the frozen biopsies, 4 10-μm-thick sections were cut and used for standard RNA isolation. After cutting, a 3-μm-thick section was stained with hematoxylin/eosin for histological examination and only tissues with more than 80% tumor cells were included. RNA was isolated with TRIzol reagent (Invitrogen) according to manufacturer's protocol. RNA was treated with DNAse and purified using the RNeasy mini-kit (Qiagen). The quality and quantity of the RNA was determined by Agilent Lab-on-Chip analysis. For labeling, 10 μg of total RNA was amplified by *in vitro* transcription using T7 RNA polymerase. Labelled RNA samples were hybridized according to a randomized design to the human genome U133 plus 2.0 microarrays (Affymetrix). The microarrays were loaded with 200 μL of hybridization cocktail solution and then placed in Genechip Hybridization Oven 640 (Affymetrix) rotating at 60 rpm at 45°C for 16 hours. After hybridization, the arrays were washed on Genechip Fluidics Station 400 (Affymetrix) and scanned using Genechip Scanner 3000 (Affymetrix)

Published OnlineFirst March 8, 2011; DOI: 10.1158/1078-0432.CCR-10-2320

according to the manufacturers' procedure. Labeling of the RNA, quality control, the microarray hybridization, and scanning were performed by ServiceXS (Leiden, http://www.serviceXS.com) according to Affymetrix standards. Preprocessing of CEL files was performed with Affymetrix Expression Console software. Probe set expression summary was done using the Robust Multi-array Average (RMA) algorithm. Quality of the microarray data was checked using histograms, box plots, and a RNA degradation plot. Principal component analysis (PCA) was performed for controlling the quality of the hybridizations (24). The MIAME-compliant microarray data are available at http://www.ncbi.nlm.nih.gov/geo/ under accession number GSE26511.

Pathway analysis

GSEA was performed with the software package GSEA 2.0, developed by the Broad Institute of MIT and Harvard (22). Each gene was ranked according to its relative difference in expression between the N_0 and N_+ group using the Student's *t* statistic. Ranked expression data for all annotated 20,606 genes (in case of more than one probe per gene, the probe with the highest intensity was considered) were compared against a large collection of biological gene sets to determine whether genes both at the top or bottom of the ranked list were enriched in these functional gene sets. GSEA analysis was performed separately with a total of 155 gene sets in the KEGG (21) and 125 gene sets in the Biocarta data base. The gene sets used are available at the Molecular Signature Database (http://www.broadinstitute.org/gsea/msigdb/). Statistical enrichment was determined using an empirical phenotype-based permutation test based on 1,000 permutations. Furthermore, for each functional set the false discovery rate (FDR) and nominal *P*- value were calculated. *P* values of less than 0.05 were considered statistically significant.

In addition, oncogenic pathway activation analysis was performed using experimentally generated expression signatures from HMECs that reflect the activation of various oncogenic signaling pathways (c-Myc, H-Ras, c-Src, E2F3, and β-catenin; ref. 23). Publicly available software implementing these models (BinReg; ref. 23) was used to assess the activation probability of the oncogenic pathways in our 39 cervical tumor samples. Principal Component Analysis (PCA) was used to correct for variances due to possible unreliable activation probabilities (24–27). The oncogenic pathway activation analysis and PCA are described in detail in the supplementary data.

Class comparison

Class comparison was performed using the software package BRB Array Tools 3.7.0, developed by the Biometric Research Branch of the US National Cancer Institute (http://linus.nci.nih.gov/BRB-ArrayTools.html). Differentially expressed probe sets were identified using a parametric 2-sample *t* test (with random variance model) with a significance threshold of $P < 0.001$. In addition, for each probe set the FDR was determined (28). Finally, a global test was performed to assess the probability of getting the observed number of identified significant probe sets by chance, that is, under the assumption that there is no difference in expression between the N_0 and N_+ group. Differentially expressed genes were ranked according to lowest FDR and lowest parametric *P* value.

Immunohistochemical validation

Immunohistochemistry of the relevant proteins (Smad2, pSmad2, Smad4, β-catenin, E-cadherin, and p120) was first performed on whole tumor slides of a small series of 20 randomly selected cervical cancer tissues (see supplementary data for more details). Only if a homogeneous staining pattern was found, immunostaining was performed on TMAs. TMAs were constructed as previously described (29). For immunohistochemistry, 3-μm sections from the TMAs were immunostained with antibodies directed against β-catenin, p120, Smad4, and pSmad2. Normal cervical epithelium was used as a positive control. Scoring was performed by 2 independent observers without knowledge of clinical data. A concordance of more than 90% was found for all stainings. The discordant cases were reviewed and scores were reassigned on consensus of opinion. Staining intensity was semiquantitatively scored as negative (0), weak positive (1), moderate positive (2), and strong positive (3). Also the percentage of positive cells was recorded. Positive Smad4 expression was defined as presence of both more than 50% moderate/strong positive nuclear and moderate/strong positive cytoplasmic staining (30). β-catenin and p120 positivity was defined as membranous staining at any intensity (1–3) in more than 50% of cells (31).

Statistical analysis was performed with SPSS 16.0 for Windows (SPSS Inc.). Associations between immunostainings and lymph node metastases were compared using logistic regression models, in which immunostainings were used as dependent factors and the clinicopathological characteristics as independent factors. *P* values of less than 0.05 were considered statistically significant.

Results

Biological pathways associated with pelvic lymph node status

GSEA using biological pathway definitions according to KEGG and Biocarta data bases revealed that 5 pathways (TGF-β, NFAT, ALK, BAD, and PAR1 pathway) were significantly enriched in the N_0 group, whereas only 1 pathway (Glycosphingolipid Biosynthesis Neo Lactoseries pathway) was enriched in the N_+ group (Table 2). The ALK pathway is defined by genes that are also present in the β-catenin and TGF-β pathways such as WNT1, CTNNB1, TGFB2, TGFR2, and SMADs (http://www.broadinstitute.org/gsea/msigdb/).

Analyzing the association between oncogenic pathways and lymph node status, using expression signatures that reflect the activation of 5 major oncogenic signaling pathways (c-Myc, H-Ras, c-Src, E2F3, and β-catenin) revealed that the activation probabilities of the oncogenic β-catenin pathway correlated highly significantly with N_+ ($P =$

Published OnlineFirst March 8, 2011; DOI: 10.1158/1078-0432.CCR-10-2320

Table 2. Results of GSEA using pathway definitions of Biocarta and KEGG

Pathway	*P*	FDR	Enriched in
NFAT (Biocarta)	0.004	0.252	N_0
ALK (Biocarta)	0.013	0.269	N_0
BAD (Biocarta)	0.016	0.492	N_0
TGF-β (KEGG)	0.027	1.000	N_0
Glycosphingolipid Biosynthesis Neo Lactoseries (KEGG)	0.039	1.000	N_+
PAR1 (Biocarta)	0.046	0.907	N_0

Abbreviation: FDR = False discovery rate

0.001). Supplementary Table 1 shows the predicted probabilities for all 5 oncogenic pathways. A scatter plot of the activation probability of β-catenin for our 39 cervical tumor samples shows that tumor samples with a low or high probability of β-catenin activation are predominantly N_0 or N_+ tumor samples, respectively (Fig. 1).

Of these 7 pathways, only the β-catenin and TGF-β pathways, or separate components within these pathways, have been implicated in metastasis or tumor progression (32–35). Therefore, in this manuscript we decided to especially validate whether these tumor cell pathways are predictive for pelvic lymph node status in early cervical cancer.

Individual genes of the β-catenin pathway are related to lymph node status

We identified probe sets that were differentially expressed between N_0 and N_+ samples using a random-variance *t* test. *P* values, fold changes, and FDRs for all 54,675 probe sets are given in Supplementary Table 2. Using this analysis, we identified 188 probe sets that are differentially expressed at a significance level of $P < 0.001$ (Table 3). The probability of finding at least 188 significant probe sets by chance, that is, under the assumption that there are no differences between the N_0 and N_+ groups was $P = 0.035$. These 188 probe sets represented 149 unique genes of which 46 genes were upregulated and 103 genes were downregulated in the N_+ group. Interestingly, 14 probe sets representing 5 unique genes (*TCF4*, *CTNNAL1*, *DKK3*, *CTNND1/p120*, and *WNT5a*) belong to the β-catenin pathway. This is in good agreement with our pathway analysis using all genes.

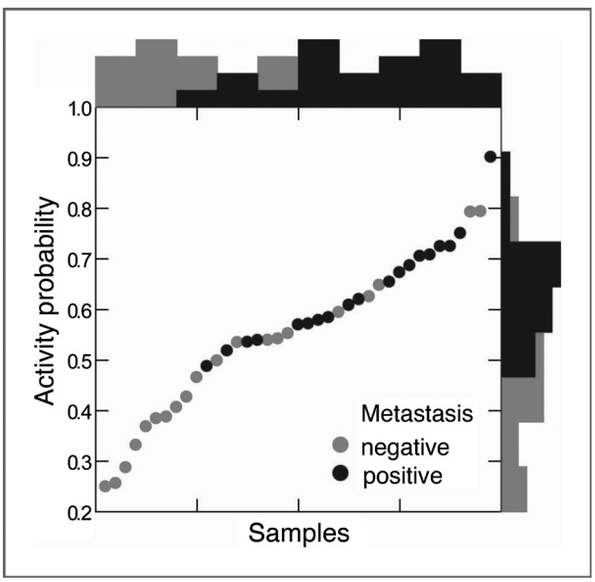

Figure 1. Scatter plot of the activation probability of β-catenin for the 39 cervical tumor samples

Immunohistochemical validation of the TGF-β and β-catenin pathway

To validate the association between the lymph node status in early-stage cervical cancer and the oncogenic TGF-β signaling and β-catenin pathways, we performed immunohistochemistry using antibodies directed against proteins that are representative of both these pathways. For this purpose, we used a series of pretreatment early-stage cervical cancer tissues of 274 patients.

Phosphorylation of Smad2/3 and concomitant translocation into the nucleus is an important step in transforming growth factor β (TGF-β) signaling and expression of Smad4 is an essential partner of Smad2/3 in the formation of transcriptional complexes (36, 37). To validate whether Smad2, pSmad2, and/or Smad4 staining on the TMA are representative for the whole tumor, first whole tumor slides of a small series of 20 randomly selected cervical cancer tissues were immunostained. This immunostaining revealed that only Smad4 staining was homogeneous (data not shown). Therefore, Smad4 staining on the TMA reflects best the staining of the whole tumor. Thirty-five out of 255 evaluable cervical carcinomas showed positive Smad4 staining (see Supplementary Fig. 1 for representative immunostainings). Univariate logistic regression analysis of various clinicopathological features revealed that Smad4 positivity was not only related to N_0, (OR: 0.20, 95% CI: 0.06–0.66) but also to infiltration depth less than 10 mm (OR: 0.35, 95% CI: 0.16–0.76; Table 4).

To validate whether β-catenin signaling is associated with presence of lymph node metastases in cervical cancer, immunohistochemical staining was performed for β-catenin, E-cadherin, and p120 on whole tumor slides of 20 cervical cancer tissues. This revealed that E-cadherin was not a homogeneous staining. Immunostaining of β-catenin, a key protein in the canonical β-catenin pathway (38), and CTNND1/p120 that is involved in noncanonical β-catenin signaling (35) and was one of the 5 β-catenin related transcripts present in the list of 149 differentially expressed genes (188 probe sets; Table 3), was therefore performed on TMAs. Positive p120 immunostaining was observed in 112 of 268 (42%) and positive β-catenin in 140 of 272 (51%) patients (see Supplementary Fig. 1 for examples). Logistic regression analysis revealed no

Published OnlineFirst March 8, 2011; DOI: 10.1158/1078-0432.CCR-10-2320

Table 3. 188 probe sets differentially expressed between N_0 samples and N_+ samples

Upregulated in N_0						
Rank	**Parametric *P* value**	**FDR**	**Fold-change**	**Probe set**	**Gene symbol**	**Description**
1	0.0000012	0.042	2.054	222146_s_at	TCF4	transcription factor 4
3	0.0000023	0.042	1.623	209250_at	DEGS1	degenerative spermatocyte homologue 1, lipid desaturase (Drosophila)
4	0.0000064	0.075	1.795	212387_at	TCF4	transcription factor 4
5	0.0000069	0.075	2.173	203753_at	TCF4	transcription factor 4
7	0.0000142	0.111	2.165	226931_at	TMTC1	transmembrane and tetratricopeptide repeat containing 1
8	0.0000168	0.115	1.979	212382_at	TCF4	transcription factor 4
9	0.0000197	0.120	1.684	232304_at	PELI1	pellino homologue 1 (Drosophila)
10	0.0000221	0.121	1.391	1559249_at	ATXN1	ataxin 1
11	0.0000264	0.125	1.556	209281_s_at	ATP2B1	ATPase, Ca++ transporting, plasma membrane 1
12	0.0000318	0.125	1.473	221683_s_at	CEP290	centrosomal protein 290kDa
13	0.0000323	0.125	2.795	226084_at	MAP1B	microtubule-associated protein 1B
15	0.0000344	0.125	1.504	212509_s_at	MXRA7	matrix-remodelling associated 7
16	0.0000414	0.127	1.807	214724_at	DIXDC1	DIX domain containing 1
17	0.0000416	0.127	1.818	212386_at	TCF4	transcription factor 4
18	0.0000429	0.127	1.791	213891_s_at	TCF4	transcription factor 4
19	0.0000445	0.127	1.571	226546_at		Not available
20	0.0000483	0.127	1.672	226676_at	ZNF521	zinc finger protein 521
21	0.0000495	0.127	2.243	227812_at	TNFRSF19	tumor necrosis factor receptor superfamily, member 19
22	0.0000513	0.127	2.269	226322_at	TMTC1	transmembrane and tetratricopeptide repeat containing 1
23	0.0000562	0.134	2.047	225946_at	RASSF8	Ras association (RalGDS/AF-6) domain family 8
24	0.0000627	0.141	1.528	235834_at	CALD1	caldesmon 1
25	0.0000655	0.141	1.786	1554007_at	ZNF483	zinc finger protein 483
26	0.0000677	0.141	1.668	231869_at	ZNF451	zinc finger protein 451
28	0.0000738	0.141	1.369	207604_s_at	SLC4A7	solute carrier family 4, sodium bicarbonate cotransporter, member 7
29	0.0000748	0.141	2.051	235599_at	LOC339535	hypothetical protein LOC339535
30	0.0000792	0.143	1.382	202126_at	PRPF4B	PRP4 pre-mRNA processing factor 4 homologue B (yeast)
31	0.0000810	0.143	1.704	235592_at	ELL2	elongation factor, RNA polymerase II, 2
32	0.0000849	0.145	1.516	208662_s_at	TTC3	tetratricopeptide repeat domain 3
34	0.0000913	0.147	1.674	209682_at	CBLB	Cas-Br-M (murine) ecotropic retroviral transforming sequence b
36	0.0000977	0.148	1.682	204466_s_at	SNCA	synuclein, alpha (non A4 component of amyloid precursor)
37	0.0001040	0.154	1.249	206862_at	ZNF254	zinc finger protein 254
38	0.0001140	0.161	1.384	202144_s_at	ADSL	adenylosuccinate lyase
39	0.0001146	0.161	1.548	225246_at	STIM2	stromal interaction molecule 2
40	0.0001243	0.170	1.504	204964_s_at	SSPN	sarcospan (Kras oncogene-associated gene)
41	0.0001274	0.170	1.341	236796_at	BACH2	BTB and CNC homology 1, basic leucine zipper transcription factor 2
42	0.0001375	0.177	1.364	206240_s_at	ZNF136	zinc finger protein 136
43	0.0001402	0.177	2.443	202468_s_at	CTNNAL1	catenin (cadherin-associated protein), alpha-like 1

Published OnlineFirst March 8, 2011; DOI: 10.1158/1078-0432.CCR-10-2320

Table 3. 188 probe sets differentially expressed between N_0 samples and N_+ samples (Cont'd)

Upregulated in N_0						
Rank	**Parametric *P* value**	**FDR**	**Fold-change**	**Probe set**	**Gene symbol**	**Description**
44	0.0001424	0.177	1.724	229307_at	ANKRD28	ankyrin repeat domain 28
46	0.0001660	0.196	1.665	214741_at	ZNF131	zinc finger protein 131
47	0.0001719	0.196	1.554	202909_at	EPM2AIP1	EPM2A (laforin) interacting protein 1
50	0.0001827	0.198	2.587	238852_at	PRRX1	paired related homeobox 1
51	0.0001846	0.198	1.892	224911_s_at	DCBLD2	discoidin, CUB and LCCL domain containing 2
52	0.0001909	0.199	1.930	214247_s_at	DKK3	dickkopf homologue 3 (Xenopus laevis)
53	0.0001927	0.199	2.111	202149_at	NEDD9	neural precursor cell expressed, developmentally down-regulated 9
54	0.0001996	0.200	1.236	242470_at	EID2B	EP300 interacting inhibitor of differentiation 2B
55	0.0002015	0.200	2.131	212190_at	SERPINE2	serpin peptidase inhibitor, clade E (nexin, plasminogen activator inhibitor type 1), member 2
58	0.0002382	0.211	1.233	225417_at	EPC1	enhancer of polycomb homologue 1 (Drosophila)
60	0.0002396	0.211	1.574	223519_at	ZAK	sterile alpha motif and leucine zipper containing kinase AZK
62	0.0002422	0.211	1.739	220145_at	MAP9	microtubule-associated protein 9
63	0.0002433	0.211	1.402	220917_s_at	WDR19	WD repeat domain 19
64	0.0002520	0.215	1.300	214078_at	PAK3	p21 (CDKN1A)-activated kinase 3
65	0.0002700	0.222	1.807	213954_at	KIAA0888	KIAA0888 protein
66	0.0002796	0.222	1.479	208993_s_at	PPIG	peptidylprolyl isomerase G (cyclophilin G)
67	0.0002799	0.222	1.433	209537_at	EXTL2	exostoses (multiple)-like 2
68	0.0002815	0.222	1.226	230212_at	SPRY1	sprouty homologue 1, antagonist of FGF signaling (Drosophila)
69	0.0002860	0.222	1.982	204359_at	FLRT2	fibronectin leucine rich transmembrane protein 2
70	0.0002868	0.222	1.370	221829_s_at	TNPO1	transportin 1
71	0.0002932	0.222	1.731	229228_at	CREB5	cAMP responsive element binding protein 5
72	0.0002936	0.222	1.606	215716_s_at	ATP2B1	ATPase, Ca++ transporting, plasma membrane 1
74	0.0003077	0.225	1.567	204422_s_at	FGF2	fibroblast growth factor 2 (basic)
76	0.0003123	0.225	1.550	202207_at	ARL4C	ADP-ribosylation factor-like 4C
77	0.0003203	0.225	1.385	225324_at	CRLS1	cardiolipin synthase 1
82	0.0003690	0.245	1.296	232064_at		Not available
84	0.0003894	0.249	1.742	219765_at	ZNF329	zinc finger protein 329
85	0.0003953	0.249	1.896	235102_x_at	GRAP	GRB2-related adaptor protein
86	0.0003955	0.249	1.451	218263_s_at	ZBED5	zinc finger, BED-type containing 5
87	0.0003998	0.249	1.661	233223_at	NEDD9	neural precursor cell expressed, developmentally down-regulated 9
88	0.0004024	0.249	1.736	212385_at	TCF4	transcription factor 4
94	0.0004467	0.249	1.372	202379_s_at	NKTR	natural killer-tumor recognition sequence
95	0.0004474	0.249	1.987	221958_s_at	GPR177	G protein-coupled receptor 177
96	0.0004563	0.249	2.021	212233_at	MAP1B	microtubule-associated protein 1B
98	0.0004632	0.249	1.470	229504_at	RAB23	RAB23, member RAS oncogene family
100	0.0004788	0.249	1.377	214212_x_at	PLEKHC1	pleckstrin homology domain containing, family C (with FERM domain) member 1
101	0.0004809	0.249	1.529	212985_at		Not available
102	0.0004847	0.249	1.319	218724_s_at	TGIF2	TGFB-induced factor homeobox 2

Published OnlineFirst March 8, 2011; DOI: 10.1158/1078-0432.CCR-10-2320

Table 3. 188 probe sets differentially expressed between N_0 samples and N_+ samples (Cont'd)

Upregulated in N_0						
Rank	**Parametric *P* value**	**FDR**	**Fold-change**	**Probe set**	**Gene symbol**	**Description**
103	0.0004848	0.249	1.681	221898_at	PDPN	podoplanin
105	0.0004878	0.249	1.358	207719_x_at	CEP170	centrosomal protein 170kDa
106	0.0004879	0.249	1.434	201363_s_at	IVNS1ABP	influenza virus NS1A binding protein
108	0.0004977	0.249	1.639	209763_at	CHRDL1	chordin-like 1
110	0.0005001	0.249	1.976	205498_at	GHR	growth hormone receptor
111	0.0005223	0.251	1.871	232113_at		Not available
115	0.0005310	0.251	1.337	215164_at	TCF4	transcription factor 4
116	0.0005320	0.251	1.783	222313_at	CNOT2	CCR4-NOT transcription complex, subunit 2
118	0.0005771	0.261	1.467	224763_at	RPL37	ribosomal protein L37
119	0.0005776	0.261	1.610	209204_at	LMO4	LIM domain only 4
120	0.0005823	0.261	1.408	227847_at	EPM2AIP1	EPM2A (laforin) interacting protein 1
121	0.0005829	0.261	1.539	208663_s_at	TTC3	tetratricopeptide repeat domain 3
122	0.0005896	0.261	1.200	230578_at	ZNF471	zinc finger protein 471
124	0.0006142	0.261	1.892	202196_s_at	DKK3	dickkopf homologue 3 (Xenopus laevis)
125	0.0006208	0.261	1.483	239768_x_at		Not available
127	0.0006305	0.261	2.216	204105_s_at	NRCAM	neuronal cell adhesion molecule
128	0.0006319	0.261	1.308	212970_at	APBB2	amyloid beta (A4) precursor protein-binding, family B, member 2
132	0.0006388	0.261	1.556	232063_x_at	FARSB	phenylalanyl-tRNA synthetase, beta subunit
133	0.0006487	0.261	2.005	220253_s_at	LRP12	low density lipoprotein-related protein 12
134	0.0006488	0.261	1.265	226843_s_at	PAPD5	PAP associated domain containing 5
135	0.0006501	0.261	1.563	211698_at	EID1	EP300 interacting inhibitor of differentiation 1
136	0.0006511	0.261	1.715	213425_at	WNT5A	wingless-type MMTV integration site family, member 5A
139	0.0006907	0.266	1.468	208661_s_at	TTC3	tetratricopeptide repeat domain 3
140	0.0006972	0.266	1.686	229530_at	GUCY1A3	guanylate cyclase 1, soluble, alpha 3
142	0.0006992	0.266	1.645	219174_at	IFT74	intraflagellar transport 74 homologue (Chlamydomonas)
143	0.0007020	0.266	2.073	209289_at	NFIB	nuclear factor I/B
144	0.0007035	0.266	1.166	210742_at	CDC14A	CDC14 cell division cycle 14 homologue A (S. cerevisiae)
145	0.0007101	0.266	1.438	209737_at	MAGI2	membrane associated guanylate kinase, WW and PDZ domain containing 2
146	0.0007116	0.266	1.931	204463_s_at	EDNRA	endothelin receptor type A
150	0.0007383	0.266	1.262	200702_s_at	DDX24	DEAD (Asp-Glu-Ala-Asp) box polypeptide 24
151	0.0007394	0.266	1.523	223463_at	RAB23	RAB23, member RAS oncogene family
152	0.0007406	0.266	1.300	225565_at	FAM119A	family with sequence similarity 119, member A
154	0.0007903	0.280	1.611	218788_s_at	SMYD3	SET and MYND domain containing 3
155	0.0007943	0.280	1.161	241002_at		Not available
156	0.0008043	0.282	1.567	235368_at	ADAMTS5	ADAM metallopeptidase with thrombospondin type 1 motif, 5 (aggrecanase-2)
157	0.0008090	0.282	4.220	211756_at	PTHLH	parathyroid hormone-like hormone
158	0.0008157	0.282	1.288	212746_s_at	CEP170	centrosomal protein 170kDa
159	0.0008251	0.282	3.270	226847_at	FST	follistatin

Published OnlineFirst March 8, 2011; DOI: 10.1158/1078-0432.CCR-10-2320

Table 3. 188 probe sets differentially expressed between N_0 samples and N_+ samples (Cont'd)

Upregulated in N_0

Rank	Parametric *P* value	FDR	Fold-change	Probe set	Gene symbol	Description
161	0.0008325	0.282	1.610	205609_at	ANGPT1	angiopoietin 1
163	0.0008462	0.282	1.559	201810_s_at	SH3BP5	SH3-domain binding protein 5 (BTK-associated)
164	0.0008593	0.282	1.412	1556543_at	ZCCHC7	zinc finger, CCHC domain containing 7
167	0.0008649	0.282	1.501	230424_at	C5orf13	chromosome 5 open reading frame 13
168	0.0008661	0.282	1.278	210438_x_at	TROVE2	TROVE domain family, member 2
169	0.0008764	0.284	1.680	205381_at	LRRC17	leucine rich repeat containing 17
170	0.0009009	0.284	2.125	209290_s_at	NFIB	nuclear factor I/B
171	0.0009055	0.284	1.745	234996_at	CALCRL	calcitonin receptor-like
173	0.0009087	0.284	2.649	230493_at	TMEM46	transmembrane protein 46
174	0.0009110	0.284	3.152	231867_at	ODZ2	odz, odd Oz/ten-m homologue 2 (Drosophila)
175	0.0009192	0.284	1.377	225735_at	ANKRD50	ankyrin repeat domain 50
176	0.0009212	0.284	1.305	219078_at	GPATCH2	G patch domain containing 2
178	0.0009236	0.284	1.507	224989_at		Not available
179	0.0009406	0.287	1.466	202150_s_at	NEDD9	neural precursor cell expressed, developmentally down-regulated 9
180	0.0009579	0.288	1.668	202133_at	WWTR1	WW domain containing transcription regulator 1
181	0.0009606	0.288	1.435	208670_s_at	EID1	EP300 interacting inhibitor of differentiation 1
182	0.0009666	0.288	1.911	204686_at	IRS1	insulin receptor substrate 1
183	0.0009670	0.288	1.434	202132_at	WWTR1	WW domain containing transcription regulator 1
184	0.0009679	0.288	1.416	225961_at	KLHDC5	kelch domain containing 5
186	0.0009892	0.289	1.329	243305_at		Not available
188	0.0009983	0.289	1.447	242300_at	UBB	ubiquitin B

Upregulated in N_+

Rank	Parametric *P* value	FDR	Fold-change	Probe set	Gene symbol	Description
2	0.0000021	0.042	0.346	220013_at	ABHD9	abhydrolase domain containing 9
6	0.0000085	0.077	0.635	223540_at	PVRL4	poliovirus receptor-related 4
14	0.0000330	0.125	0.766	239377_at	MGC11102	hypothetical protein MGC11102
27	0.0000703	0.141	0.760	204188_s_at	RARG	retinoic acid receptor, gamma
33	0.0000876	0.145	0.767	208104_s_at	TSC22D4	TSC22 domain family, member 4
35	0.0000959	0.148	0.738	239825_at	ATF6	activating transcription factor 6
45	0.0001493	0.181	0.785	212147_at	SMG5	Smg-5 homologue, nonsense mediated mRNA decay factor (C. elegans)
48	0.0001721	0.196	0.749	218928_s_at	SLC37A1	solute carrier family 37 (glycerol-3-phosphate transporter), member 1
49	0.0001775	0.198	0.646	205204_at	NMB	neuromedin B
56	0.0002063	0.201	0.620	238804_at		Not available
57	0.0002209	0.211	0.702	209679_s_at	LOC57228	small trans-membrane and glycosylated protein
59	0.0002395	0.211	0.760	210678_s_at	AGPAT2	1-acylglycerol-3-phosphate O-acyltransferase 2 (lysophosphatidic acid acyltransferase, beta)

Published OnlineFirst March 8, 2011; DOI: 10.1158/1078-0432.CCR-10-2320

Table 3. 188 probe sets differentially expressed between N_0 samples and N_+ samples (Cont'd)

Upregulated in N_0						
Rank	**Parametric *P* value**	**FDR**	**Fold-change**	**Probe set**	**Gene symbol**	**Description**
61	0.0002421	0.211	0.837	215106_at	TTC22	tetratricopeptide repeat domain 22
73	0.0002965	0.222	0.821	235234_at	FLJ36874	FLJ36874 protein
75	0.0003083	0.225	0.205	213240_s_at	KRT4	keratin 4
78	0.0003206	0.225	0.755	237063_at		Not available
79	0.0003300	0.228	0.847	220335_x_at	CES3	carboxylesterase 3 (brain)
80	0.0003346	0.229	0.805	239230_at	HES5	hairy and enhancer of split 5 (Drosophila)
81	0.0003464	0.234	0.636	209261_s_at	NR2F6	nuclear receptor subfamily 2, group F, member 6
83	0.0003720	0.245	0.615	1557944_s_at	CTNND1	catenin (cadherin-associated protein), delta 1
89	0.0004172	0.249	0.707	229493_at	HOXD9	homeobox D9
90	0.0004215	0.249	0.851	236676_at	NUDCD3	NudC domain containing 3
91	0.0004255	0.249	0.756	206949_s_at	RUSC1	RUN and SH3 domain containing 1
92	0.0004286	0.249	0.648	235871_at	LIPH	lipase, member H
93	0.0004387	0.249	0.666	205977_s_at	EPHA1	EPH receptor A1
97	0.0004607	0.249	0.757	1555784_s_at	IRAK1	interleukin-1 receptor-associated kinase 1
99	0.0004724	0.249	0.744	220599_s_at	CARD14	caspase recruitment domain family, member 14
104	0.0004856	0.249	0.838	207566_at	MR1	major histocompatibility complex, class I-related
107	0.0004928	0.249	0.857	1563147_at		Not available
109	0.0004986	0.249	0.662	211240_x_at	CTNND1	catenin (cadherin-associated protein), delta 1
112	0.0005283	0.251	0.784	231788_at	GPR92	G protein-coupled receptor 92
113	0.0005286	0.251	0.790	236725_at	WWC1	WW and C2 domain containing 1
114	0.0005291	0.251	0.799	232608_x_at	CARD14	caspase recruitment domain family, member 14
117	0.0005408	0.253	0.554	1553611_s_at	FLJ33790	hypothetical protein FLJ33790
123	0.0006007	0.261	0.828	218749_s_at	SLC24A6	solute carrier family 24 (sodium/potassium/calcium exchanger), member 6
126	0.0006225	0.261	0.422	206595_at	CST6	cystatin E/M
129	0.0006343	0.261	0.778	1553072_at	BNIPL	BCL2/adenovirus E1B 19kD interacting protein like
130	0.0006354	0.261	0.678	222809_x_at	C14orf65	chromosome 14 open reading frame 65
131	0.0006384	0.261	0.712	207525_s_at	GIPC1	GIPC PDZ domain containing family, member 1
137	0.0006534	0.261	0.828	231248_at	CST6	cystatin E/M
138	0.0006787	0.266	0.655	220289_s_at	AIM1L	absent in melanoma 1-like
141	0.0006973	0.266	0.813	1487_at	ESRRA	estrogen-related receptor alpha
147	0.0007208	0.266	0.701	203918_at	PCDH1	protocadherin 1
148	0.0007290	0.266	0.776	204827_s_at	CCNF	cyclin F
149	0.0007310	0.266	0.626	216010_x_at	FUT3	fucosyltransferase 3 (galactoside 3(4)-L-fucosyltransferase, Lewis blood group)
153	0.0007781	0.278	0.845	220962_s_at	PADI1	peptidyl arginine deiminase, type I
160	0.0008325	0.282	0.678	230252_at	GPR92	G protein-coupled receptor 92
162	0.0008440	0.282	0.748	236616_at		Not available
165	0.0008616	0.282	0.695	235988_at	GPR110	G protein-coupled receptor 110

Published OnlineFirst March 8, 2011; DOI: 10.1158/1078-0432.CCR-10-2320

Table 3. 188 probe sets differentially expressed between N_0 samples and N_+ samples (Cont'd)

Upregulated in N_0						
Rank	**Parametric *P* value**	**FDR**	**Fold-change**	**Probe set**	**Gene symbol**	**Description**
166	0.0008645	0.282	0.645	1552685_a_at	GRHL1	grainyhead-like 1 (Drosophila)
172	0.0009064	0.284	0.280	203757_s_at	CEACAM6	carcinoembryonic antigen-related cell adhesion molecule 6 (non-specific cross reacting antigen)
177	0.0009227	0.284	0.724	235095_at	CCDC64B	coiled-coil domain containing 64B
185	0.0009826	0.289	0.873	233154_at	AFF3	AF4/FMR2 family, member 3
187	0.0009963	0.289	0.696	226638_at	ARHGAP23	Rho GTPase activating protein 23

association between β-catenin protein expression and presence of lymph node metastases (Table 4). However, positive p120 staining was associated with N_+ (OR: 1.79, 95% CI: 1.05–3.05), in agreement with our microarray results.

Discussion

In the present study, pathways associated with pelvic lymph node metastases in 39 (20 N_0 and 19 N_+) early-stage cervical cancer patients were identified. Our analysis of well-known and novel ($n = 285$) pathway signatures revealed an association of lymph node metastases with only few gene sets or signatures, including 2 well-known oncogenic biological gene sets. Enrichment of the TGF-β pathway was related to N_0, whereas oncogenic pathway activation of β-catenin was associated with N_+ patients. The association of both the TGF-β and the β-catenin signaling pathway with lymph node metastases was validated in a large consecutive series of early-stage cervical cancer patients by immunohistochemistry. Immunostaining of Smad4 and p120 representing the TGF-β and β-catenin signaling pathway, respectively, confirmed the association with lymph node metastasis in early-stage cervical cancer.

Until now, all studies using microarray platforms for differentiating between patient with and without lymph node metastases in cervical cancer focused on gene profiles and individual genes present in these profiles (14–17). Another approach is to identify biological pathways that are involved in biological differences between cancers, using pathway analysis methods on all genes that are differentially expressed between 2 phenotypes. For example, Lagarde and colleagues identified pathways that differentiated between N_0 and N_+ esophageal adenocarcinomas (39). Furthermore, Crijns and colleagues identified pathways contributing to clinical outcome of serous ovarian cancer (24). Interestingly, many of these pathways were known for being important in carcinogenesis or cancer progression, which indicates the strength of this approach. To our knowledge, we are the first to identify pathways for discriminating between N_0 and N_+ cervical cancer patients using pathway analysis methods.

Our analysis showed that TGF-β is one of the most important pathways affecting the metastatic potential in early-stage cervical cancer. First, of all 280 tested unique pathways (from the KEGG and Biocarta data bases), the TGF-β pathway was significantly enriched in N_0 (Table 2). Binding of the TGF-β ligand to its receptors initiates intracellular signaling by phosphorylation of Smad2 and Smad3. These phosphorylated Smads then bind to Smad4 and translocate into the nucleus, where this Smad complex is involved in regulation of gene transcription (36, 37). Immunostaining using Smad4 of 255 early-stage cervical carcinomas confirmed that TGF-β pathway activation was related to absence of lymph node metastases. Although Smad4 is a key protein in TGF-β signaling (36, 37), it is not known whether Smad4 immunostaining is representative of TGF-β signaling activity throughput. Immunostaining of more members of the TGF-β pathway would enhance our results, however no homogeneous staining was found for Smad2 and pSmad2 and therefore these stainings could not be performed on TMAs. Early in carcinogenesis, the TGF-β pathway contributes to tumor suppression, for example by stimulating apoptosis and inhibition of growth (36, 37) However, later in the process of tumor progression or in invasive cancer, oncogenic activity of TGF-β signaling is predominantly present, including increased migration and invasiveness, which may result in metastases. This transition from a tumor suppressor to an oncogenic pathway can be due to various alterations in TGF-β signaling, such as loss of Smad signaling and activation of Smad-independent, more oncogenic pathways, such as MAPK pathways (36, 37). Furthermore, TGF-β is directly involved in the formation of metastases, as it contributes to the establishment and outgrowth of lung and bone metastases in breast cancer models (32, 34). Smad4 downregulation is associated with TGF-β downregulation and has been implicated in cervical cancer (30) and metastatic mouse models (32). The downregulation of Smad4 in N_+ is consistent with these data and establishes TGF-β as one of the pathways affecting the metastatic potential in early-stage cervical cancer.

In addition to the TGF-β pathway, GSEA revealed that the NFAT, ALK, BAD, and PAR1 pathways are significantly

Published OnlineFirst March 8, 2011; DOI: 10.1158/1078-0432.CCR-10-2320

Table 4. Logistic regression analysis for the relation between clinicopathological characteristics and stainings

Smad4 ($n = 255$)	Smad4–		Smad4+		Smad4 positive OR (95% CI)
	n/total	%	*n*/total	%	
Age (continuous)					1.00 (0.98–1.03)
Age ≥43	111/220	50%	21/35	60%	
Stage ≥Ib2	83/220	38%	11/35	31%	0.76 (0.35–1.62)
SCC	150/206	73%	20/31	65%	0.68 (0.31–1.51)
Poor differentiation	87/216	40%	17/34	50%	1.48 (0.72–3.06)
Lymphangioinvasion	119/220	54%	15/35	43%	0.64 (0.31–1.31)
Infiltration depth ≥10 mm	111/207	54%	10/35	29%	**0.35 (0.16–0.76)**
Tumor diameter ≥4 cm	65/220	30%	6/35	17%	0.49 (0.20–1.24)
Positive lymph nodes	71/220	32%	3/35	9%	**0.20 (0.06–0.66)**
p120 ($n = 268$)	**p120–**		**p120+**		**p120 positive**
	***n*/total**	**%**	***n*/total**	**%**	**OR (95% CI)**
Age (continuous)					1.00 (0.98–1.02)
Age ≥43	78/156	50%	60/112	54%	
Stage ≥Ib2	58/156	37%	40/112	36%	0.94 (0.57–1.56)
SCC	88/142	62%	90/108	83%	**3.07 (1.67–5.64)**
Poor differentiation	64/153	42%	41/110	37%	0.83 (0.50–1.37)
Lymphangioinvasion	70/156	45%	68/112	61%	**1.90 (1.16–3.11)**
Infiltration depth ≥10 mm	70/147	48%	54/108	50%	1.10 (0.67–1.81)
Tumor diameter ≥4 cm	44/156	28%	31/112	28%	0.97 (0.57–1.67)
Positive lymph nodes	37/156	24%	40/112	36%	**1.79 (1.05–3.05)**
β-catenin ($n = 272$)	**β-catenin–**		**β-catenin+**		**β-catenin positive**
	***n*/total**	**%**	***n*/total**	**%**	**OR (95% CI)**
Age (continuous)					1.01 (0.99–1.03)
Age ≥43	63/132	48%	76/140	54%	
Stage ≥Ib2	48/132	36%	52/140	37%	1.03 (0.63–1.69)
SCC	81/126	64%	101/129	78%	**2.00 (1.15–3.49)**
Poor differentiation	52/132	39%	53/135	39%	0.99 (0.61–1.62)
Lymphangioinvasion	63/132	48%	77/140	55%	1.34 (0.83–2.16)
Infiltration depth ≥10 mm	64/125	51%	61/134	46%	0.80 (0.49–1.30)
Tumor diameter ≥4 cm	38/132	29%	38/140	27%	0.92 (0.54–1.57)
Positive lymph nodes	37/132	28%	43/140	31%	1.14 (0.67–1.92)

NOTE: Bold signifies $P < 0.05$

SCC = squamous cell carcinoma

The proportion of patients with less than 2 representative tissue cores varied from 1%–7%

enriched in the N_0 group and the Glycosphingolipid Biosynthesis Neo Lactoseries pathway in the N_+ group (Table 2). Presently, we and others have not characterized these pathways in detail for their possible association with the metastatic behavior of tumor cells. However, as these 5 pathways are also significantly associated with lymph node status, more detailed analysis is warranted to confirm their possible role in lymph node metastasis in early-stage cervical cancer.

A limitation of GSEA is that pathway activation can not be assessed for an individual patient. Therefore, another strategy was developed in which expression signatures are experimentally generated to reflect activation status of various oncogenic signaling pathways (23). This pathway

Published OnlineFirst March 8, 2011; DOI: 10.1158/1078-0432.CCR-10-2320

analysis indicates that N_+ patients had a higher probability of β-catenin pathway activation than N_0 patients, pointing to a role for the β-catenin pathway in formation of lymph node metastases (Fig. 1). Interestingly, the gene set of 188 differentially expressed probe sets between N_0 and N_+, included 5 unique genes involved in the β-catenin-pathway including *p120 (CTNND1* or *catenin delta 1*), *CTNNAL1* (*catenin alpha-like 1*), *DKK3* (*dickkopf homologue 3*), *WNT5a*, and *TCF4* (*transcription factor 4*), but did not include β-catenin. In good agreement with these findings, immunohistochemistry confirmed the association of p120 and the lack of correlation of β-catenin with N_+. β-catenin is an important member of both the WNT-signaling pathway and the cell–cell adhesion pathway. However, immunohistochemical analysis revealed no relation between β-catenin and lymph node metastases, which is in agreement with other studies (31, 40) and indicates that the canonical Wnt/β-catenin pathway (containing β-catenin, Wnt1, APC) is not involved in mediating the invasive potential in cervical cancer. In normal cervical epithelium, β-catenin is involved in E-cadherin mediated cell–cell adhesion, by binding to the cytoplasmic domain of E-cadherin. Loss of E-cadherin causes disruption of cell adhesion and therefore might contribute to metastases (35, 38). P120 (also referred to as CTNND1 or delta-catenin) is a member of the catenin family and was originally reported to stabilize the cadherin-complex by direct interaction with the proximal domain of E-cadherin (35, 38). On the other hand, p120 (especially p120 isoform 1) promotes cell motility and invasiveness in cancer (33). P120 was reported to exert its effects by modulating the activities of Rho GTPases, for example by inhibiting activity of RhoA and activation of Rac and Cdc42 (33, 41). To our knowledge our study is the first that reports that p120 expression is associated with presence of lymph node metastases in early-stage cervical cancer. The link of p120 to Rho GTPases in activating the metastatic potential might also offer new opportunities for therapy, as invasion has been inhibited successfully using Rho-inhibitors (42).

Thus, both the TGF-β and the p120-associated noncanonical β-catenin pathway are related to lymph node metastases in cervical cancer. This indicates an important role for epithelial to mesenchymal transition (EMT), as both pathways may contribute to EMT. EMT is characterized by loss of the epithelial phenotype of cells and cells adopt a mesenchymal phenotype. It can be induced by alterations in TGF-β signaling, such as loss of Smad4 (43) and EMT is characterized by loss of E-cadherin, with disruption of cell adhesion as a consequence. Furthermore, EMT results in increased motility of cells, and increased invasion. All these processes contribute to the formation of metastases (44, 45). TGF-β signaling and β-catenin also cooperate in EMT. Loss of E-cadherin causes increased β-catenin signaling, which cooperates with autocrine TGF-β signaling to maintain an mesenchymal phenotype (46). Thus, deregulation of both the TGF-β and the β-catenin pathway, as observed in our study, indicates a role for EMT in lymph node metastasis in cervical cancer. Interestingly, miR-200a which is known for inhibition of TGF-β-mediated EMT by maintaining the epithelial phenotype through regulating expression of the E-cadherin transcriptional repressors ZEB1 and ZEB2 (47), was found to be a suppressor of metastasis in cervical cancer (48). This supports the importance of EMT in lymph node metastasis in cervical cancer.

Presence of lymph node metastases is still one of the most important factors in the choice of treatment for early-stage cervical cancer patients. No markers are currently available for accurate prediction of lymph node metastases before primary surgery. By evaluation of the primary tumor, expression levels of proteins such as Smad4 and p120 as representatives for the TGF-β signaling and β-catenin pathway, respectively, also cannot accurately predict presence of pelvic lymph node metastasis. However, more detailed analysis of these pathways might result in the identification of additional markers that will increase the clinical sensitivity en specificity. More importantly, by identifying pathways involved in lymph node metastasis in early-stage cervical cancer, new opportunities for pathway targeted therapy can be considered to inhibit the metastatic potential, as reported for both pathways (49, 50).

Disclosure of Potential Conflicts of Interest

No potential conflicts of interest were disclosed.

Grant Support

Dutch Cancer Society (project number RUG 2004-3161). P.D. Moerland acknowledges support by the BioRange programme of The Netherlands Bioinformatics Centre (NBIC), supported by a BSIK grant through the Netherlands Genomics Initiative (NGI). EVLvT was supported by the FP6 European Union Project "Peroxisome" (LSHG-CT-2004-512018).

The costs of publication of this article were defrayed in part by the payment of page charges. This article must therefore be hereby marked *advertisement* in accordance with 18 U.S.C. Section 1734 solely to indicate this fact.

Received August 30, 2010; revised December 17, 2010; accepted December 29, 2010; published OnlineFirst March 8, 2011.

References

1. Creasman WT, Kohler MF. Is lymph vascular space involvement an independent prognostic factor in early cervical cancer?Gynecol Oncol 2004;92:525–9.
2. Sakuragi N. Up-to-date management of lymph node metastasis and the role of tailored lymphadenectomy in cervical cancer. Int J Clin Oncol 2007;12:165–75.
3. Landoni F, Maneo A, Colombo A, Placa F, Milani R, Perego P, et al. Randomised study of radical surgery versus radiotherapy for stage Ib-IIa cervical cancer. Lancet 1997;350:535–40.
4. Sevin BU, Nadji M, Lampe B, Lu Y, Hilsenbeck S, Koechli OR, et al. Prognostic factors of early stage cervical cancer treated by radical hysterectomy. Cancer 1995;76:1978–86.
5. van de Putte G, Holm R, Lie AK, Trope CG, Kristensen GB. Expression of p27, p21, and p16 protein in early squamous cervical cancer and its relation to prognosis. Gynecol Oncol 2003;89:140–7.
6. Lee IJ, Park KR, Lee KK, Song JS, Lee KG, Lee JY, et al. Prognostic value of vascular endothelial growth factor in Stage IB carcinoma of the uterine cervix. Int J Radiat Oncol Biol Phys 2002;54:768–79.

Published OnlineFirst March 8, 2011; DOI: 10.1158/1078-0432.CCR-10-2320

7. Gortzak-Uzan L, Jimenez W, Nofech-Mozes S, Ismiil N, Khalifa MA, Dubé V, et al. Sentinel lymph node biopsy vs. pelvic lymphadenectomy in early stage cervical cancer: is it time to change the gold standard?Gynecol Oncol 2010;116:28–32.
8. Chambers AF, Groom AC, MacDonald IC. Dissemination and growth of cancer cells in metastatic sites. Nat Rev Cancer 2002;2:563–72.
9. Molloy T, van't Veer LJ. Recent advances in metastasis research. Curr Opin Genet Dev 2008;18:35–41.
10. van't Veer LJ, Dai H, van de Vijver MJ, He YD, Hart AA, Mao M, et al. Gene expression profiling predicts clinical outcome of breast cancer. Nature 2002;415:530–6.
11. Beer DG, Kardia SL, Huang CC, Giordano TJ, Levin AM, Misek DE, et al. Gene-expression profiles predict survival of patients with lung adenocarcinoma. Nat Med 2002;8:816–24.
12. Roepman P, Wessels LF, Kettelarij N, Kemmeren P, Miles AJ, Lijnzaad P, et al. An expression profile for diagnosis of lymph node metastases from primary head and neck squamous cell carcinomas. Nat Genet 2005;37:182–6.
13. Kwon HC, Kim SH, Roh MS, Kim JS, Lee HS, Choi HJ, et al. Gene expression profiling in lymph node-positive and lymph node-negative colorectal cancer. Dis Colon Rectum 2004;47:141–52.
14. Biewenga P, Buist MR, Moerland PD, Ver Loren van Themaat E, van Kampen AH, ten Kate FJ, et al. Gene expression in early stage cervical cancer. Gynecol Oncol 2008;108:520–6.
15. Lyng H, Brvig RS, Svendsrud DH, Holm R, Kaalhus O, Knutstad K, et al. Gene expressions and copy numbers associated with metastatic phenotypes of uterine cervical cancer. BMC Genomics 2006;7:268.
16. Grigsby PW, Watson M, Powell MA, Zhang Z, Rader JS. Gene expression patterns in advanced human cervical cancer. Int J Gynecol Cancer 2006;16:562–7.
17. Kim TJ, Choi JJ, Kim WY, Choi CH, Lee JW, Bae DS, et al. Gene expression profiling for the prediction of lymph node metastasis in patients with cervical cancer. Cancer Sci 2008;99:31–8.
18. Draghici S, Khatri P, Eklund AC, Szallasi Z. Reliability and reproducibility issues in DNA microarray measurements. Trends Genet 2006;22:101–9.
19. Jarvinen AK, Hautaniemi S, Edgren H, Auvinen P, Saarela J, Kallioniemi OP, et al. Are data from different gene expression microarray platforms comparable?Genomics 2004;83:1164–8.
20. Ransohoff DF. Rules of evidence for cancer molecular-marker discovery and validation. Nat Rev Cancer 2004;4:309–14.
21. Kanehisa M, Araki M, Goto S, Hattori M, Hirakawa M, Itoh M, et al. KEGG for linking genomes to life and the environment. Nucleic Acids Res 2008;36:D480–4.
22. Subramanian A, Tamayo P, Mootha VK, Mukherjee S, Ebert BL, Gillette MA, et al. Gene set enrichment analysis: a knowledge-based approach for interpreting genome-wide expression profiles. Proc Natl Acad Sci U S A 2005;102:15545–50.
23. Bild AH, Yao G, Chang JT, Wang Q, Potti A, Chasse D, et al. Oncogenic pathway signatures in human cancers as a guide to targeted therapies. Nature 2006;439:353–7.
24. Crijns AP, Fehrmann RS, de JS, Gerbens F, Meersma GJ, Klip HG, et al. Survival-related profile, pathways, and transcription factors in ovarian cancer. PLoS Med 2009;6:e24.
25. Scotlandi K, Remondini D, Castellani G, Manara MC, Nardi F, Cantiani L, et al. Overcoming resistance to conventional drugs in Ewing sarcoma and identification of molecular predictors of outcome. J Clin Oncol 2009;27:2209–16.
26. Sherlock G. Analysis of large-scale gene expression data. Brief Bioinform 2001;2:350–62.
27. Alter O, Brown PO, Botstein D. Singular value decomposition for genome-wide expression data processing and modeling. Proc Natl Acad Sci U S A 2000;97:10101–6.
28. Benjamini Y, Hochberg Y. Controlling the false discovery rate: a practical and powerful approach to multiple testing. J R Statist Soc B 1995;57:289–300.
29. Noordhuis MG, Eijsink JJ, ten Hoor KA, Roossink F, Hollema H, Arts HJ, et al. Expression of epidermal growth factor receptor (EGFR) and activated EGFR predict poor response to (chemo) radiation and survival in cervical cancer. Clin Cancer Res 2009;15:7389–97.
30. Kloth JN, Kenter GG, Spijker HS, Uljee S, Corver WE, Jordanova ES, et al. Expression of Smad2 and Smad4 in cervical cancer: absent nuclear Smad4 expression correlates with poor survival. Mod Pathol 2008;21:866–75.
31. Van de Putte G, Kristensen GB, Baekelandt M, Lie AK, Holm R. E-cadherin and catenins in early squamous cervical carcinoma. Gynecol Oncol 2004;94:521–7.
32. Padua D, Zhang XH, Wang Q, Nadal C, Gerald WL, Gomis RR, et al. TGFbeta primes breast tumors for lung metastasis seeding through angiopoietin-like 4. Cell 2008;133:66–77.
33. Yanagisawa M, Huveldt D, Kreinest P, Lohse CM, Cheville JC, Parker AS, et al. A p120 catenin isoform switch affects Rho activity, induces tumor cell invasion, and predicts metastatic disease. J Biol Chem 2008;283:18344–54.
34. Mourskaia AA, Dong Z, Ng S, Banville M, Zwaagstra JC, O'Connor-McCourt MD, et al. Transforming growth factor-beta1 is the predominant isoform required for breast cancer cell outgrowth in bone. Oncogene 2009;28:1005–15.
35. Wheelock MJ, Johnson KR. Cadherin-mediated cellular signaling. Curr Opin Cell Biol 2003;15:509–14.
36. Elliott RL, Blobe GC. Role of transforming growth factor Beta in human cancer. J Clin Oncol 2005;23:2078–93.
37. Jakowlew SB. Transforming growth factor-beta in cancer and metastasis. Cancer Metastasis Rev 2006;25:435–57.
38. Nelson WJ, Nusse R. Convergence of Wnt, beta-catenin, and cadherin pathways. Science 2004;303:1483–7.
39. Lagarde SM, Ver Loren van Themaat PE, Moerland PD, Gilhuijs-Pederson LA, Ten Kate FJ, Reitsma PH, et al. Analysis of gene expression identifies differentially expressed genes and pathways associated with lymphatic dissemination in patients with adenocarcinoma of the esophagus. Ann Surg Oncol 2008;15:3459–70.
40. Imura J, Ichikawa K, Takeda J, Fujimori T. Beta-catenin expression as a prognostic indicator in cervical adenocarcinoma. Int J Mol Med 2001;8:353–8.
41. Reynolds AB, Roczniak-Ferguson A. Emerging roles for p120-catenin in cell adhesion and cancer. Oncogene 2004;23:7947–56.
42. Fritz G, Kaina B. Rho GTPases: promising cellular targets for novel anticancer drugs. Curr Cancer Drug Targets 2006;6:1–14.
43. Zhao S, Venkatasubbarao K, Lazor JW, Sperry J, Jin C, Cao L, et al. Inhibition of STAT3 Tyr705 phosphorylation by Smad4 suppresses transforming growth factor beta-mediated invasion and metastasis in pancreatic cancer cells. Cancer Res 2008;68:4221–8.
44. Thiery JP. Epithelial-mesenchymal transitions in development and pathologies. Curr Opin Cell Biol 2003;15:740–6.
45. Rees JR, Onwuegbusi BA, Save VE, Alderson D, Fitzgerald RC. In vivo and in vitro evidence for transforming growth factor-beta1-mediated epithelial to mesenchymal transition in esophageal adenocarcinoma. Cancer Res 2006;66:9583–90.
46. Eger A, Stockinger A, Park J, Langkopf E, Mikula M, Gotzmann J, et al. Beta-catenin and TGFbeta signalling cooperate to maintain a mesenchymal phenotype after FosER-induced epithelial to mesenchymal transition. Oncogene 2004;23:2672–80.
47. Gregory PA, Bert AG, Paterson EL, Barry SC, Tsykin A, Farshid G, et al. The miR-200 family and miR-205 regulate epithelial to mesenchymal transition by targeting ZEB1 and SIP1. Nat Cell Biol 2008;10:593–601.
48. Hu X, Schwarz JK, Lewis JS Jr., Huettner PC, Rader JS, Deasy JO, et al. A microRNA expression signature for cervical cancer prognosis. Cancer Res 2010;70:1441–8.
49. Dihlmann S, von Knebel DM. Wnt/beta-catenin-pathway as a molecular target for future anti-cancer therapeutics. Int J Cancer 2005;113:515–24.
50. Nagaraj NS, Datta PK. Targeting the transforming growth factor-beta signaling pathway in human cancer. Expert Opin Investig Drugs 2010;19:77–91.

Published OnlineFirst March 8, 2011; DOI: 10.1158/1078-0432.CCR-10-2320

Clinical Cancer Research

Involvement of the TGF-β and β-Catenin Pathways in Pelvic Lymph Node Metastasis in Early-Stage Cervical Cancer

Maartje G. Noordhuis, Rudolf S.N. Fehrmann, G. Bea A. Wisman, et al.

Clin Cancer Res 2011;17:1317-1330. Published OnlineFirst March 8, 2011.